JOURNAL OF SOLID STATE CHEMISTRY **131,** 101–107 (1997)
ARTICLE NO. SC977354

Structural and Luminescence Properties of $Ca_{1-x}La_xS$ ($x = 0–0.3$)

Han Choi, Chang-Hong Kim,* and Chong-Hong Pyun

Division of Applied Science, Korea Institute of Science and Technology, P.O. Box 131, Seoul 130-650, Korea

and

Sung-Jin Kim

Department of Chemistry, Ewha Womans University, Seoul 120-750, Korea

Received October 7, 1996; in revised form February 17, 1997; accepted February 18, 1997

The structure and photoluminescence of $Ca_{1-x}La_xS$ ($x=0–0.3$) were investigated. The samples were prepared by sulfurizing the mixture of $CaCO_3$ and La_2O_3 in the flux of Na_2CO_3–S or K_2CO_3–S, and by gas reaction with CS_2. By using different methods of preparation, defect structure and concentration could be controlled chemically. $Ca_{1-x}La_xS$ prepared in the Na_2CO_3–S flux has a wider solid solution range than that prepared in the K_2CO_3–S flux, and such a feature seems to be due to similar ionic size of Na^+ and Ca^{2+}. As the substitution of La^{3+} increases, the band gap of the host material decreases due to the increase of the lattice parameters, and the photoluminescence spectra of the $Ca_{1-x}La_xS$ shift to longer wavelengths. Since La^{3+} ion itself is transparent to ultraviolet radiation, vacancies ($V_{Ca^{2+}}$, $V_{S^{2+}}$) and substituted ions ($Na^+_{Ca^{2+}}$, $La^{3+}_{Ca^{2+}}$) seem to be associated with luminescence centers. The acceptor levels of $Na^+_{Ca^{2+}}$ and $V_{Ca^{2+}}$ are estimated to be about 1.1 and 0.5 eV above the valence band, respectively, and the donor levels of $La^{3+}_{Ca^{2+}}$ and $V_{S^{2-}}$ to be about 1.8 eV below the conduction band. The emission bands observed at 500–580 nm suggest the recombination processes of donors with acceptors.

INTRODUCTION

Alkaline-earth sulfides are known as excellent host materials for the cathodo-, photo-, thermo-, and electroluminescence phosphors (1–5). Especially, rare-earth doped CaS instead of ZnS has recently attracted interest from investigators because of their high dielectric constant and lattice constant. Some of them show good blue emission and have a potential as phosphors for device application such as multicolor thin film electroluminescence. Also, it is well known that solid solutions of CaS with rare-earth sulfides (Y_2S_3, Dy_2S_3, Er_2S_3) have high melting points and chemical stability (6), thus they have been widely used as solid electrolytes (7, 8).

Alkaline-earth sulfides are usually prepared by heating the alkaline-earth salts in H_2S or CS_2 atmosphere or by sulfurizing with Na_2CO_3–S flux (9, 10). Many researchers reported that CaS can be substituted with various activators or activator–coactivator pairs, which produce the luminescence (11, 12). Generally, when monovalent or trivalent ions are substituted as activators, alkaline metal ions and halides can be used as coactivators for charge compensation.

Extensive studies for various activators and coactivators including group IA, IIA metals, early transition metal ions, and halides in CaS were carried out (13–15). Most of the previous studies concentrated on atomic transition of activators. However, comparatively little effort has been directed toward rare-earth activators with no *d* and *f* energy levels. Since Y^{3+} and La^{3+} themselves have no *d* and *f* electronic emission level, the various vacancies and defects of host materials likely contribute to complicated luminescence centers (16) as electron donors and acceptors. The recombination processes of donors and acceptors have been described by Schon-Klasens (17) and Prener-Williams in alkaline-earth sulfides (18–20). However, the effect of different synthetic methods on the luminescence centers, thus on luminescence spectra, has not been studied.

In this paper the range of solid solution and the nature of the luminescence center of $Ca_{1-x}La_xS$ prepared in two flux materials (Na_2CO_3–S and K_2CO_3–S) were investigated. The structural effect on luminescence spectra and the role of intrinsic and extrinsic defects in CaS governing the useful physical properties is investigated. The energy level of defects and vacancies influenced by the change of the lattice parameter of $Ca_{1-x}La_xS$ was discussed.

0022-4596/97 $25.00

EXPERIMENTS

$Ca_{1-x}La_xS$ was prepared in the sulfurizing fluxes of alkaline carbonate (Na_2CO_3–S and K_2CO_3–S) and sulfur mixture. The starting materials used were $CaCO_3$ (Aldrich, + 99%), La_2O_3 (Shin-Etsu, 99.99%), and sulfurizing fluxes. All starting materials were used without purification. The starting materials were well mixed and heated in a covered alumina crucible at 1000°C for 2 hrs. The residual flux in the product was washed out with distilled water at room temperature, and the final product was dried after rinsing with ethyl alcohol.

The solid solution of $Ca_{1-x}La_xS$ by gas reaction was prepared by heating the mixture of $CaCO_3$ and La_2O_3 at 1000°C for 7 hrs in a mixed stream of CS_2 and N_2.

The product phases were analyzed by X-ray diffraction technique, and the Rietveld-type analysis was carried out for detailed structural information. X-ray diffraction patterns were recorded with a Norelco X-ray diffractometer using Cu$K\alpha$ radiation. For photoluminescence measurements, a monochromated 150 W Xenon lamp was used as an excitation source. The photoluminescence spectra were obtained using a monochromator-equipped photomultiplier tube.

Diffused absorption spectra of phosphors were obtained using a Carry 2200 UV-VIS spectrophotometer with $BaSO_4$ as a reference.

The content of cations in the products was determined by atomic absorption analysis (AA) and inductively coupled plasma–mass spectrometry (ICP-MS).

RESULTS AND DISCUSSION

1. X-ray Diffraction Study

The X-ray diffraction patterns of $Ca_{1-x}La_xS$ prepared in the Na_2CO_3–S flux are shown in Fig. 1a. As the La^{3+} content in the reaction mixture is increased, intensities of all odd number reflections (for example, 111 reflection) of CaS increase, and all peak positions shift to lower angles. The changes of X-ray patterns indicate that as La^{3+} ions are substituted to Ca^{2+} sites in CaS, the lattice parameters are increased. The diffraction peaks from the La_2O_2S phase appear when the concentration of La^{3+} is above $x = 0.3$.

Figure 1b shows X-ray diffraction patterns of $Ca_{1-x}La_xS$ prepared in the K_2CO_3–S flux. The La_2O_2S phase is observed above $x = 0.1$ in the reaction mixture, which indicates that more La^{3+} can be substituted for CaS in the Na_2CO_3–S flux than in the K_2CO_3–S flux.

Figure 1c shows X-ray diffraction patterns of $Ca_{1-x}La_xS$ prepared under CS_2/N_2 flow. In the gas reaction, the $CaLa_2S_4$ phase appeared above $x = 0.03$ in the reaction mixture and became major phase at $x = 0.7$, indicating a very low limit of solid solution of $Ca_{1-x}La_xS$. $CaLa_2S_4$ has Th_3P_4-type ($a = 8.686$ Å) structure, and in this structure

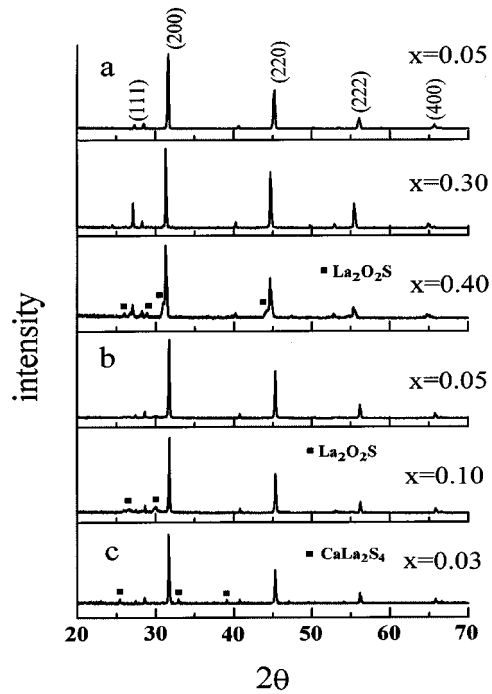

FIG. 1. XRD of $Ca_{1-x}La_xS$ prepared in (a) Na_2CO_3–S flux, (b) K_2CO_3–S flux, and (c) CS_2/N_2 gas reaction.

25% of metal vacancies are randomly distributed in the lattice (8, 21). Since there is no compensating cations in the reaction mixture, one Ca^{2+} vacant site may be produced in CaS for two La^{3+} ion substitution ($3Ca^{2+} = 2La^{3+}_{Ca^{2+}} + V_{Ca^{2+}}$).

Figure 2 shows a change of lattice parameter of CaS with La^{3+} content prepared in the two fluxes. Lattice parameters of $Ca_{1-x}La_xS$ prepared in the Na_2CO_3–S flux increased linearly from 5.70 to 5.77 Å following Vegard's law. However, the lattice parameters of $Ca_{1-x}La_xS$ prepared in the

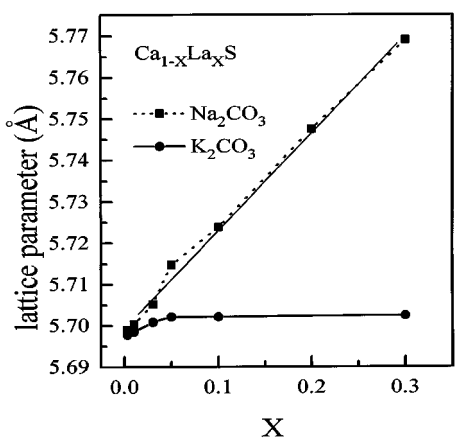

FIG. 2. Lattice parameter change of $Ca_{1-x}La_xS$ with La^{3+} substitution prepared in the fluxes (Na_2CO_3–S, K_2CO_3–S).

K_2CO_3–S flux do not change so much as those prepared in the Na_2CO_3–S flux. Since the ionic size of K^+(1.38 Å) is much larger than that of Ca^{2+}(1.00 Å) (22), it is more difficult for the K^+–La^{3+} pair than the Na^+–La^{3+} pair to be substituted on two Ca^{2+} sites.

In the X-ray pattern, the intensity ratio of (111) to (200) reflection is strongly dependent on the concentration of substituted La^{3+} ions on the Ca^{2+} site. Since scattering factors of f_{La} and f_{Ca} are so different, the intensities of all the odd *hkl* reflections increase relative to all the even *hkl* reflections on the substitution of Ca^{2+} ions to La^{3+} ions. For CaS prepared in the Na_2CO_3–S flux, the observed intensity ratio of $I(1\,1\,1)/I(2\,0\,0)$ agreed with the calculated ratio up to $x = 0.3$. But the intensity ratios of $I(1\,1\,1)/I(2\,0\,0)$ increase slightly with La^{3+} substitution up to $x = 0.05$ (added concentration of La^{3+}) for the CaS prepared in the K_2CO_3 flux and are constant above it, which suggest a narrow range (below $x = 0.05$) of solid solution. The calculated intensity ratios of $I(1\,1\,1)/I(2\,0\,0)$ are shown in Fig. 3. Figure 4 shows one of the results of Rietveld analysis for $Ca_{1-x}La_xS$ prepared in the Na_2CO_3–S flux. Rietveld refinement was carried out to obtain the scale factor, zero point, back ground parameters, thermal parameters, cell parameters, and atomic positions and occupancies (Table 1).

The Na^+ or K^+ in $Ca_{1-x}La_xS$ powders was analyzed by AA and ICP-MS methods, and the results are shown in Table 2. The concentration ratio of Na^+ to La^{3+} was almost unity. It indicates that two Ca^{2+} sites are easily replaced by La^{3+}(1.03 Å) and Na^+(1.02 Å) due to the similar ionic size (22). Thus, $Ca_{1-x}La_xS$ prepared in the Na_2CO_3–S flux can be expressed as $(1-2x)$ CaS–x La_2S_3–x Na_2S. Singh *et al.* (12) reported that CaS phosphors are doped with monovalent or trivalent ions in combination with charge-compensating ions. Lehman (11) used K^+ ion as a charge compensating ion in CaS. However, the result of our analysis showed that the molar ratio of K^+ to La^{3+} in the samples from K_2CO_3–S flux is less than unity.

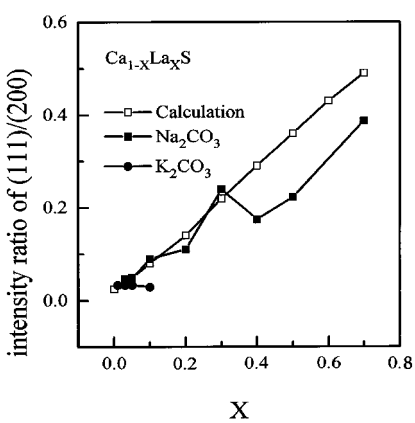

FIG. 3. The XRD intensity ratio of $I(1\,1\,1)/I(2\,0\,0)$ of $Ca_{1-x}La_xS$.

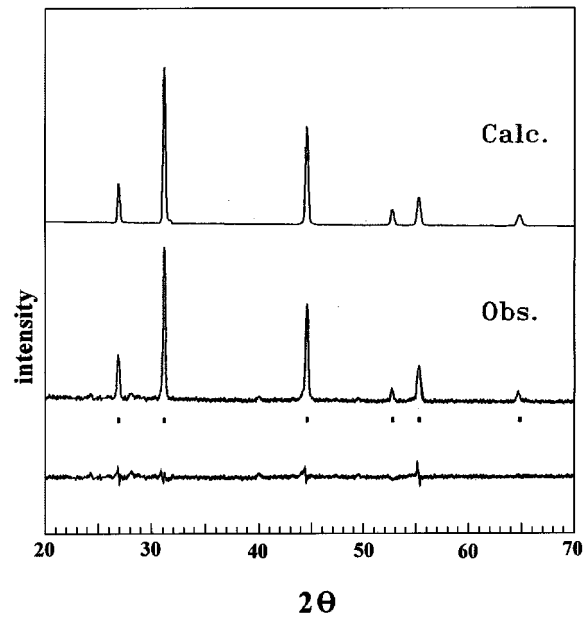

FIG. 4. The results of Rietveld analysis of $Ca_{1-x}La_xS$ ($x = 0.3$) powder diffraction. The upper pattern represents the calculated, and the lower pattern represents the observed. Vertical strokes indicate calculated Bragg peak positions. The bottom line represents the difference pattern.

The concentration of K^+ is nearly the same even though the concentration of La^{3+} increases from $x = 1.00 \times 10^{-3}$ to $x = 1.06 \times 10^{-1}$. It means that La^{3+} substitution in CaS is only up to $x = 0.05$ and La_2O_2S appears above $x = 0.05$. Since the radius of K^+ ion (1.38 Å) is much larger than that of Ca^{2+} ion (1.00 Å) (12), the replacement of Ca^{2+} by K^+ seems to be more difficult. It suggests that size effect is as important as charge effect in the replacement. Nevertheless, the concentration of K^+ doped in $Ca_{1-x}La_xS$ is smaller than that of La^{3+}, and the excess La^{3+} may be doped into CaS forming equal amounts of vacancies for charge compensation ($3Ca^{2+} = 2La^{3+}_{Ca^{2+}} + V_{Ca^{2+}}$).

TABLE 1
Refined Unit Cell and Atomic Parameters in $Fm\bar{3}m$

Atom	Site	x	y	z	Occupancy (%)	Thermal (Å)
Ca	4a	0	0	0	70(1)	0.513(2)
La	4a	0	0	0	29(1)	0.513(2)
S	4b	1/2	1/2	1/2	100(1)	0.513(2)

Symmetry	Cubic
a, b, c (Å)	5.7691(2)
β (°)	90°
Space group	$Fm\bar{3}m$ (No. 225)
Radiation	Cu$K\alpha$
R_p, R_{wp}	6.47%, 8.73%

TABLE 2
Chemical Analysis of La, Na, and K in $Ca_{1-x}La_xS$

	Na_2CO_3		K_2CO_3	
x	La[a]	Na[b]	La[a]	K[b]
0	·	1.70×10^{-3}	·	1.80×10^{-3}
0.001	1.90×10^{-3}	4.10×10^{-3}	1.00×10^{-3}	4.60×10^{-3}
0.03	2.84×10^{-2}	2.96×10^{-2}	2.95×10^{-2}	5.30×10^{-3}
0.1	9.58×10^{-2}	7.52×10^{-2}	1.06×10^{-1}	5.50×10^{-3}
0.3	2.94×10^{-1}	2.34×10^{-1}		

Note. x: input x value of La.
[a] ICP-MS.
[b] AA.

2. Photoluminescence

The excitation and emission spectra of pure CaS and Na- and K-substituted CaS are shown in Fig. 5. Pure CaS was obtained by H_2S gas reaction with $CaCO_3$, and Na- or K-substituted CaS was obtained by the reaction with $CaCO_3$ in the Na_2CO_3–S or the K_2CO_3–S flux, respectively. Pure CaS has one excitation band at 260 nm and one emission band at 450 nm. Pure CaS may have intrinsic defects of $V_{Ca^{2+}}$ and $V_{S^{2-}}$; thus, the bands at 260 and 450 nm can be assigned to the edge absorption and the transition from the trapped electron in the intrinsic $V_{S^{2-}}$ level to the valence band, respectively.

The excitation spectra of Na- and K-substituted CaS have peaks at 300 and 350 nm in addition to the edge absorption. Na- or K-substituted CaS may have extrinsic defects of $Na^{+}_{Ca^{2+}}$ or $K^{+}_{Ca^{2+}}$ which may act as an acceptor in addition to the intrinsic defects. Thus, the excitation peak at 300 nm may be associated with the excitation of electrons from the $V_{Ca^{2+}}$ level to the conduction band and that at 350 nm with the excitation of electrons from the $Na^{+}_{Ca^{2+}}$ level to the conduction level. The intensity of the edge absorption for K-substituted CaS is much higher than that for Na-substituted CaS. The emission spectra of Na- and K-substituted CaS have a band at 500 nm and a very weak shoulder at 580 nm. These emission bands at 500 and 580 nm might be assigned to the recombination of trapped electrons in $V_{S^{2-}}$ levels with holes at $Na^{+}_{Ca^{2+}}$ and $V_{Ca^{2+}}$ levels, respectively.

Reflection spectra were measured to obtain the band gap of CaS in terms of La^{3+} substitution. Diffused absorption spectra $\{F(R)\}$ were obtained from the reflection spectra by using the Kubelka–Munk function (23):

$$F(R) = (1 - R)^2/2R = K/S,$$

where R, K, and S are the reflectivity, the absorption coefficient, and the scattering coefficient, respectively. The diffused absorption spectra obtained are shown in Fig. 6 for

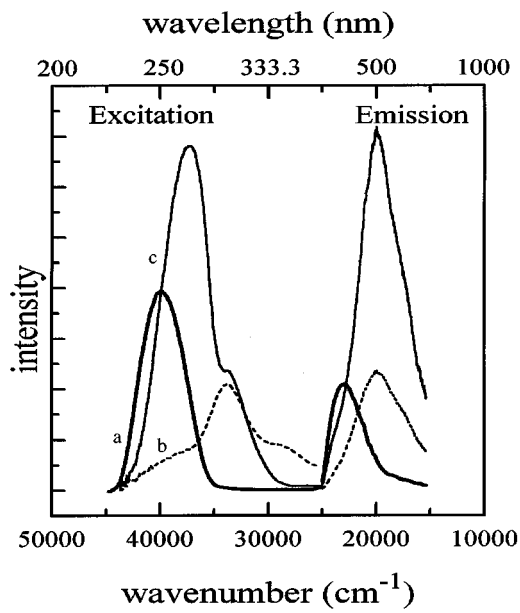

FIG. 5. Excitation and emission spectra of (a) pure CaS (H_2S), (b) Na-substituted CaS (Na_2CO_3–S), and (c) K-substituted CaS (K_2CO_3–S). Excitation spectra were obtained by monitoring the emission at 450 nm for (a) and 500 nm for (b) and (c), respectively. Emission spectra were obtained under excitation at 260 nm for (a) and 300 nm for (b) and (c).

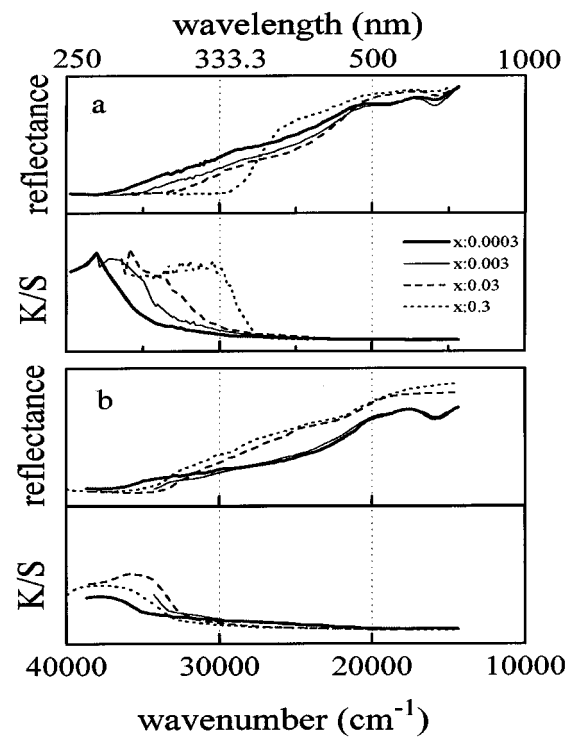

FIG. 6. Diffused absorption spectra of $Ca_{1-x}La_xS$ prepared in (a) Na_2CO_3–S flux and (b) K_2CO_3–S flux.

$Ca_{1-x}La_xS$ prepared in the fluxes. For $Ca_{1-x}La_xS$ prepared in Na_2CO_3–S flux, the edge absorption shifted toward longer wavelengths with the substitution of La^{3+}, but the absorption edge of $Ca_{1-x}La_xS$ prepared in the K_2CO_3–S flux showed similar tendency with slight shift as in the Na_2CO_3–S flux. This absorption edge shift suggests a decrease in the band gap due to the lattice parameter increase. In the previous work, similar features were also observed in series of MgS, CaS, and SrS (19). When the lattice parameter increases from MgS to SrS (MgS, 5.20 Å; CaS, 5.69 Å; and SrS, 6.03 Å), the band gap decreases in that order (MgS, 5.4 eV; CaS, 4.6 eV; and SrS, 4.4 eV) (19).

The excitation and emission spectra of $Ca_{1-x}La_xS$ prepared in the Na_2CO_3–S flux are shown in Fig. 7. The excitation spectra show different patterns depending on La^{3+} substitution. As the La^{3+} substitution increases from $x = 0.0003$ to 0.03, the edge absorption decreases and the excitation from the $V_{Ca^{2+}}$ level to the conduction band increases. Upon further increases of La^{3+} concentration to $x = 0.3$, both the edge absorption and the excitation from the $V_{Ca^{2+}}$ level decrease, while the excitation from $Na^{+}_{Ca^{2+}}$ level becomes dominant. As the La^{3+} substitution increases, so does the Na^{+} substitution for charge compensation and the excitation of the acceptors ($Na^{+}_{Ca^{2+}}$). Figure 8 shows wavenumber of excitation peak vs lattice parameter of

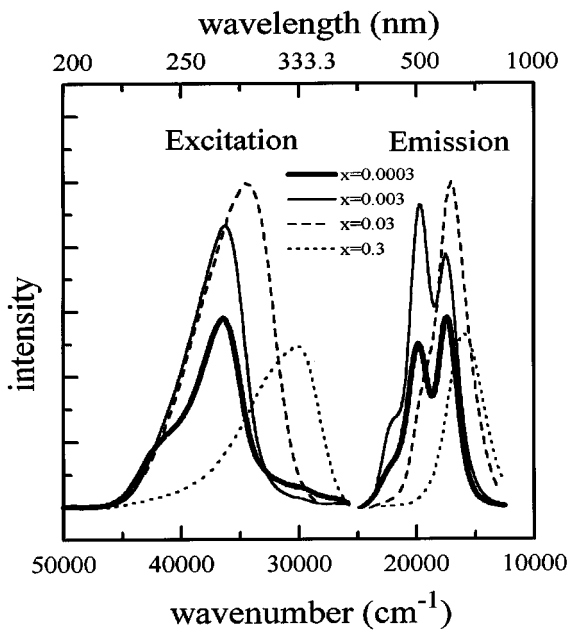

FIG. 7. Excitation and emission spectra of $Ca_{1-x}La_xS$ prepared in Na_2CO_3–S flux. Excitation spectra were obtained by monitoring the emission at 580 nm for $x = 0.0003$, 510 nm for $x = 0.003$, 585 nm for $x = 0.03$, and 630 nm for $x = 0.3$, respectively. Emission spectra were obtained under excitation at 275 nm for $x = 0.0003$ and $x = 0.003$, 290 nm for $x = 0.03$, and 330 nm for $x = 0.3$, respectively.

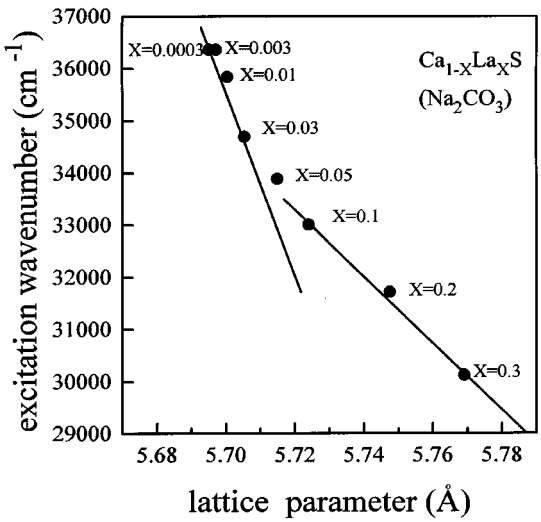

FIG. 8. The wavenumber of excitation peak vs lattice parameter of $Ca_{1-x}La_xS$ prepared in Na_2CO_3–S flux.

$Ca_{1-x}La_xS$, and it shows clearly two patterns of peak shift as the substitution of La^{3+}.

The emission spectrum of CaS at low La^{3+} substitution ($x = 0.0003$) has three dominant bands at 450, 500, and 580 nm. All the bands in the spectrum shift to the longer wavelength as the La^{3+} substitution increases from $x = 0.0003$ to $x = 0.3$. At a high La^{3+} substitution ($x = 0.3$), the spectrum shows only one band at 625 nm. The red shift of the emission spectrum has the same tendency as the excitation spectrum. This might also be due to the increase of the lattice parameter with the La^{3+} substitution. When Na^{+} and La^{3+} are codoped in CaS, there may be two kinds of extrinsic defects as $La^{3+}_{Ca^{2+}}$ and $Na^{+}_{Ca^{2+}}$. Thus, the trapped electrons in the donor levels ($La^{3+}_{Ca^{2+}}$, $V_{S^{2-}}$) may recombine with acceptors ($V_{Ca^{2+}}$, $Na^{+}_{Ca^{2+}}$). Since the emission at 580 nm increases higher, as the La^{3+} substitution becomes higher, this band may be associated with the recombination of $La^{3+}_{Ca^{2+}}$ donor with $Na^{+}_{Ca^{2+}}$ acceptor. Meanwhile, the band at 500 and 450 nm may be associated with the recombination of $La^{3+}_{Ca^{2+}}$ donor with $V_{Ca^{2+}}$ acceptor and with holes in the valence band, respectively.

Thus, the following defect equations can be proposed to interpret the excitation and emission bands when Ca^{2+} sites in CaS are replaced by La^{3+} and Na^{+}:

$$2Ca^{2+} = 2Na^{+}_{Ca^{2+}} + V_{S^{2-}}$$

$$3Ca^{2+} = 2La^{3+}_{Ca^{2+}} + V_{Ca^{2+}}$$

$$2Ca^{2+} = La^{3+}_{Ca^{2+}} + Na^{+}_{Ca^{2+}}$$

The $La^{3+}_{Ca^{2+}}$ and $V_{S^{2-}}$ are incorporated as donors and the $Na^{+}_{Ca^{2+}}$ and $V_{Ca^{2+}}$ as acceptors in CaS. Matsui *et al.* (24) also

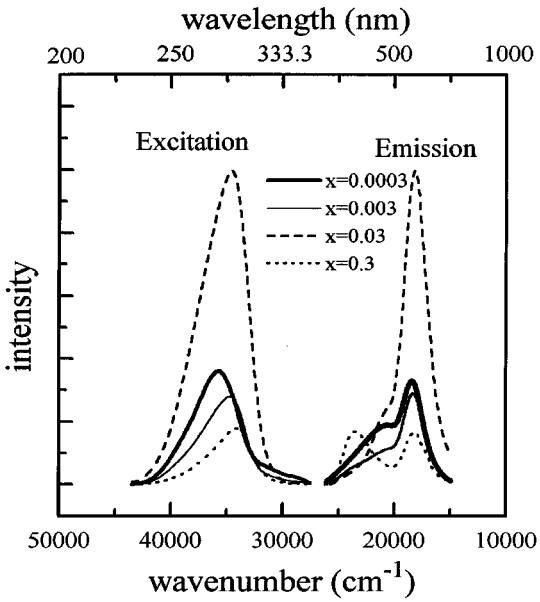

FIG. 9. Excitation and emission spectra of $Ca_{1-x}La_xS$ prepared in K_2CO_3–S flux. Excitation spectra were obtained by monitoring the emission at 580 nm. Emission spectra were obtained under excitation at 280 nm for $x = 0.0003$ and 290 nm for $x = 0.003$, 0.03, and 0.3.

reported lattice defects of $Ce^{3+}_{Ca^{2+}}$, $Cl^{-}_{S^{2-}}$, and $V_{S^{2-}}$ as donors, and $Na^{+}_{Ca^{2+}}$, $V_{Ca^{2+}}$ as acceptors in CaS:Ce^{3+}.

Emission and excitation spectra of $Ca_{1-x}La_xS$ prepared in K_2CO_3–S flux are shown in Fig. 9. These spectra have similar features as in Fig. 7 with small shift. The maximum intensity of the excitation and emission spectra was observed at $x = 0.03$.

The emission spectra of $Ca_{1-x}La_xS$ prepared in both sulfur fluxes are similar at low substitution of La^{3+} (Fig. 7 and Fig. 9): emission intensities at 450 and 500 nm decrease, while that of 580 nm increases as the substitution of La^{3+} increases. The number of intrinsic defects ($V_{Ca^{2+}}$, $V_{S^{2-}}$) may decrease as the substitution of La^{3+} increases. Since the solubility of K^+ in CaS which is prepared in the K_2CO_3–S flux is low, and the lattice parameter does not increase so much as in the case of the Na_2CO_3–S flux, the emission bands at 450, 500, and 580 nm do not shift so much.

Based on the results of our luminescence experiments, the recombination process and the energy level diagram in the band gap of CaS can be summarized as in Fig. 10. From the emission spectra and the energy level diagram, donor levels of $La^{3+}_{Ca^{2+}}$ and $V_{S^{2-}}$ are estimated to be located at around 1.8 eV below the conduction level, and the acceptor levels of $Na^{+}_{Ca^{2+}}$ and $V_{Ca^{2+}}$ are at around 1.1 and 0.5 eV above the valence band, respectively.

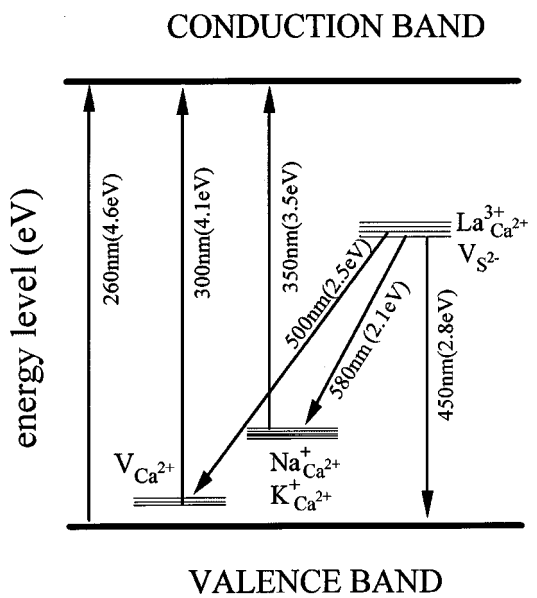

FIG. 10. Proposed energy level diagram of $Ca_{1-x}La_xS$.

CONCLUSIONS

$Ca_{1-x}La_xS$ prepared in Na_2CO_3–S flux has a wider solid solution range than that in K_2CO_3–S flux, and such a feature seems to be due to the similar ionic radius of Na^+ and Ca^{2+}. As the substitution of La^{3+} is increased in CaS, the band gap decreases due to the increased lattice parameters. Thus, photoluminescence spectra of the $Ca_{1-x}La_xS$ shift to longer wavelengths. Since the La^{3+} ion itself does not absorb ultraviolet radiation, the various vacancies ($V_{Ca^{2+}}$,$V_{S^{2-}}$) and defects ($Na^{+}_{Ca^{2+}}$, $La^{3+}_{Ca^{2+}}$) seem to be associated with the luminescence centers. Judging from the photoluminescence, the acceptor levels of $Na^{+}_{Ca^{2+}}$ and $V_{Ca^{2+}}$ could be located at about 1.1 and 0.5 eV above the valence band, respectively, and the donor levels of $La^{3+}_{Ca^{2+}}$ and $V_{S^{2-}}$ are located at 1.8 eV below the conduction band. The emission spectra observed in range 500–580 nm suggest the recombination processes between donors and acceptors. These defect structures may be applied to the preparation of efficient blue phosphor for displays by controlling the concentration of donor levels and modifying donor levels of the CaS crystal.

ACKNOWLEDGMENT

S.-J. Kim acknowledges financial support from the Korean Science and Engineering Foundation (961-0306-063-1).

REFERENCES

1. A. Wachtel, *J. Electrochem. Soc.* **107,** 199 (1960).
2. S. Bhushan and F. S. Chandra, *J. Phys. D*: *Appl. Phys.* **17,** 589 (1984).
3. B. T. Collins and M. Ling, *J. Electrochem. Soc.* **140,** 1752 (1993).

4. W. Lehmann and F. M. Ryan, *J. Electrochem. Soc.* **118,** 477 (1971).
5. R. P. Rao, *J. Mater. Sci.* 21, 3357 (1986).
6. H. L. Tsai and P. J. Meschter, *J. Electrochem. Soc.* **128,** 2229 (1981).
7. M. Sato, N. Imanaka, G. Adachi, and J. Shiokawa, *Mater. Res. Bull.* **16,** 215 (1981).
8. T. Toide, T. Utsunomiya, Y. Hoshino, and M. Sato, *Bull. Tokyo Inst. Technol.* **126,** 35 (1975).
9. S. Yokono, T. Abe, and T. Hoshina, *J. Phys. Soc. Jpn.* **46,** 351 (1979).
10. M. Pham-Thi and G. Ravaux, *J. Electrochem. Soc.* **138,** 1103 (1991).
11. W. Lehmann, *J. Lumin.* **5,** 87 (1972).
12. N. Singh, L. Marwaha, and V. K. Mathur, *Phys. Status Solidi A* **66,** 761 (1981).
13. S. Asano and N. Yamashita, *Phys. Status Solidi B* **97,** 311 (1980).
14. A. G. J. Green, B. Ray, I. V. F. Viney, and J. W. Brightwell, *Phys. Status Solidi A* **110,** 269 (1988).
15. A. M. Rastogi and S. L. Mor, *Phys. Status Solidi A* **63,** 75 (1981).
16. R. Pandey and J. H. Harding, *Philos. Mag. B* **49,** 135 (1984).
17. Y. Nakanishi, K. Natsume, Y. Fukuda, G. Shimaoka, H. Tatsuoka, H. Kuwabara, and E. Nakazawa, *J. Cryst. Growth* **101,** 462 (1990).
18. U. K. Mishira, S. L. Mor, and J. D. Ranade, *Indian J. Pure Appl. Phys.* **18,** 6 (1980).
19. W. Lehmann, *J. Electrochem. Soc.* **117,** 1389 (1970).
20. N. Yamashita and S. Asano, *J. Phys. Soc. Jpn.* **40,** 144 (1976).
21. W. H. Zachariasen, *Acta Crystallogr.* **2,** 57 (1949).
22. R. D. Shannon, *Acta Crystallogr. Sect. A* **32,** 751 (1976).
23. N. Yamashita, *J. Phys. Soc. Jpn.* **35,** 1089 (1973).
24. H. Matsui, G. Hashizume, H. Okamoto, and G. Adachi, *J. Electrochem. Soc.* **137,** 1642 (1990).